SAE TECHNICAL
PAPER SERIES

970360

Spray Combustion and Emissions in a Direct-Injection Two Stroke Engine With Wall-Stabilization of an Air-Assisted Spray

Mark V. Casarella, Marc L. Syvertsen, Jay K. Martin, Jeffrey A. Hoffman, and Jaal B. Ghandhi
University of Wisconsin-Madison

Sam W. Coates
Mercury Marine Division, Brunswick Corp.

Frank A. McGinnity
Outboard Marine Corp.

SAE The Engineering Society For Advancing Mobility Land Sea Air and Space®
INTERNATIONAL

International Congress & Exposition
Detroit, Michigan
February 24-27, 1997

400 Commonwealth Drive, Warrendale, PA 15096-0001 U.S.A. Tel: (412)776-4841 Fax:(412)776-5760

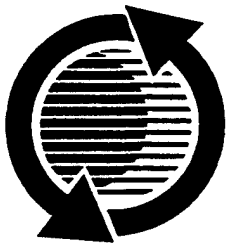

ISSN 0148-7191

Printed in USA

REPORT DOCUMENTATION PAGE

Form Approved
OMB NO. 0704-0188

1. AGENCY USE ONLY *(Leave blank)*	2. REPORT DATE	3. REPORT TYPE AND DATES COVERED
		REPRINT

4. TITLE AND SUBTITLE

TITLE ON REPRINT

5. FUNDING NUMBERS

DAAL03-92-G-0122

6. AUTHOR(S)

AUTHOR(S) ON REPRINT

7. PERFORMING ORGANIZATION NAMES(S) AND ADDRESS(ES)

UNIVERSITY OF WISCONSIN - MADISON
MADISON, WI 53706

8. PERFORMING ORGANIZATION REPORT NUMBER

9. SPONSORING / MONITORING AGENCY NAME(S) AND ADDRESS(ES)

U.S. Army Research Office
P.O. Box 12211
Research Triangle Park,, NC 27709-2211

10. SPONSORING / MONITORING AGENCY REPORT NUMBER

ARO 30340.75-EG-URI

11. SUPPLEMENTARY NOTES

The views, opinions and/or findings contained in this report are those of the author(s) and should not be construed as an official Department of the Army position, policy or decision, unless so designated by other documentation.

12a. DISTRIBUTION / AVAILABILITY STATEMENT

Approved for public release; distribution unlimited.

12 b. DISTRIBUTION CODE

13. ABSTRACT *(Maximum 200 words)*

ABSTRACT ON REPRINT

14. SUBJECT TERMS

15. NUMBER IF PAGES

16. PRICE CODE

17. SECURITY CLASSIFICATION OR REPORT	18. SECURITY CLASSIFICATION OF THIS PAGE	19. SECURITY CLASSIFICATION OF ABSTRACT	20. LIMITATION OF ABSTRACT
UNCLASSIFIED	UNCLASSIFIED	UNCLASSIFIED	UL

970360

Spray Combustion and Emissions in a Direct-Injection Two Stroke Engine With Wall-Stabilization of an Air-Assisted Spray

Mark V. Casarella, Marc L. Syvertsen, Jay K. Martin, Jeffrey A. Hoffman, and Jaal B. Ghandhi
University of Wisconsin-Madison

Sam W. Coates
Mercury Marine Division, Brunswick Corp.

Frank A. McGinnity
Outboard Marine Corp.

ABSTRACT

Previous experiments using an air-assisted spray in a two-stroke direct-injected engine demonstrated a significant improvement in combustion stability at part-load conditions when a wide injection spray was used. It was hypothesized that the decrease in variability was due to the spray following the combustion chamber wall, making it less affected by variations in the in-cylinder gas flows.

For this study, experiments were conducted to investigate engine spray combustion for cases where engine performance was not dominated by cyclic variation. Combustion and emission performance data was collected for a wide range of injection timings at several speed/load conditions. Experimental data for combustion shows that combustion stability is relatively unaffected by injection timing changes over a 40 to 100 degree window, and tolerant to spark gap projections over a range of 0.7 to 5.2 mm, depending on operating conditions. However, exhaust emissions are much more sensitive to injection timing. Spray characterization data shows that the air/fuel mixture exiting the injector tends to follow the hemispherical chamber walls, concentrating the fuel mass on the perimeter. The range of injection timings used resulted in air/fuel mixtures which should have had significant differences in the state of the mixture at the time of combustion.

INTRODUCTION

An ideal study of direct-injection two-stroke spark-ignition engine combustion and emissions would be a study in which the effects observed as a result of combustion stability were readily identifiable and able to be separated from the effects observed as a result of injection timing, spray characteristics, ignition system characteristics, or in-cylinder gas flow. Previous experiments in a single cylinder research engine operating at a part-load condition utilizing an air-assisted injector showed improved combustion stability for a wide cone angle spray which followed the chamber walls, as compared to a narrow penetrating spray [1]*. In that set of experiments, the wide spray pattern was obtained by adjusting the exit of the injector poppet such that it was slightly protruding from the wall of the combustion chamber. As the spray exited, the Coanda effect would force the fuel-air jet to be pulled toward the combustion chamber wall [2]. To generate the narrow spray, the injector was retracted further into the head so that when the fuel-air jet exited the poppet it impinged on the inner surface of the mounting hole. The fuel-air jet is deflected inward generating a narrow cone angle. It is believed that the improved stability with the wide spray was caused primarily as a result of the interaction with the wall, thus decreasing the sensitivity of the spray plume to variations in the in-cylinder bulk flow.

These observations of combustion behavior with the wide spray led to the set of experiments described in this study. In particular, it was observed in additional testing that acceptable combustion stability occurred over a wide range of injection timings. In addition, combustion stability was not strongly affected by spark electrode location. These performance characteristics then allowed for an examination of combustion behavior and engine emissions where the observations were not dominated by effects caused by combustion stability, but instead were a result of the combustion regime taking place in the engine. The range of injection timings used in this study are such that the effects of the amount of mixing and nature of the mixing process were important to the observed behavior.

EXPERIMENTAL EQUIPMENT AND ANALYSIS TOOLS

A single cylinder, two stroke, loop-scavenged, water-cooled research engine built by Mercury Marine was used for these studies, with specifications shown in Table 1. The engine is crankcase scavenged. Oil is injected into the crankcase just upstream of the reed valves to provide lubrication for the engine when operating with direct fuel injection. The cylinder head contains a hemispherical cup, with the injector located at the top of the hemisphere. Both the head cup and the injector are aligned with the cylinder axis. The spark plug is mounted on the side of the cup at a 35 degree angle from the cylinder axis, and the pressure transducer is mounted at 90 degrees tangential to the spark plug. Further details regarding this engine test cell are described in Ref. 3.

It is important to note that the engine test cell and experimental equipment were designed to study the

* Numbers in brackets designate references numbered in the Reference List.

Table 1 -Engine Specifications

Bore	85.8 mm
Stroke	67.3 mm
Connecting Rod Length	139.7 mm
Exhaust Port Timing	40.6 mm (85 °BTDC)
Intake Port Timing	52.3 mm (110 °BTDC)
Displacement	389 cm^3
Rated Speed	5000 RPM
Rated Power	19.9 kW
Combustion Chamber Volume	32.3 cm^3
Geometric Compression Ratio	11.2
True Compression Ratio	7.4

combustion process for two-stroke direct-injection engines. It was not intended for certification purposes or to prove the performance of specific systems. The absolute value of the results produced (emissions levels, combustion performance) are not likely to be indicative of what a production engine would produce. However, the trends observed, as well as the general information regarding processes controlling emissions and efficiency, are expected to be applicable to other two-stroke direct-injection engines.

An air-forced injector (AFI) developed by Ford Motor Company was used for this study. The development of this injector has been described by Schechter and Levin [2]. The injector performance has been characterized both in a high pressure chamber [4,5] and in engine experiments at Princeton University [6,7]. The injector consists of a cavity, to which fuel and air are delivered by electronically controlled solenoids, a spring-mounted outwardly opening poppet, and a vent port. An injection event begins by opening the fuel solenoid to inject fuel from a rail at a pressure of 275 kPa into the injector body. The volume of the fuel injected is small compared to the chamber volume so the chamber pressure remains constant. Following the closing of the fuel solenoid, the air solenoid is opened, and air from a rail at a pressure of 689 kPa enters the injector body. As the air flows into the injector, the pressure of the internal chamber increases until the pressure differential acting on the poppet forces it opens. The high speed flow of air atomizes the fuel as it flows past the spring loaded poppet into the combustion chamber. Following air solenoid closure, the injector body pressure decreases until the spring force on the poppet overcomes the pressure force and injection is completed. After the poppet closes the injector chamber is vented to atmospheric pressure to allow consistent recharging of fuel. A hall effect sensor is used to measure the needle lift motion inside the injector. For this experiment, the vented residual fuel vapor and air was not measured and, therefore, the mass of fuel and air injected into the engine cylinder is not known through direct measurements of fuel flow.

For this study, the wide spray configuration was used. The injector was mounted such that the exit plane of the poppet was flush with the combustion chamber wall. Thus, as the fuel/air mixture exits the injector, the Coanda effect between the spray and combustion chamber wall induces the spray to conform to the chamber wall. Figure 1 is a strobe-lit photograph of the spray pattern with the injector mounted in the cylinder head. The photograph was taken from beneath the head, looking up at an angle to the axis of the cylinder which, for imaging purposes, was acrylic. The edge of the hemispherical cup is observable as the inner-most ellipse, and the fuel spray can be seen to be following along this surface.

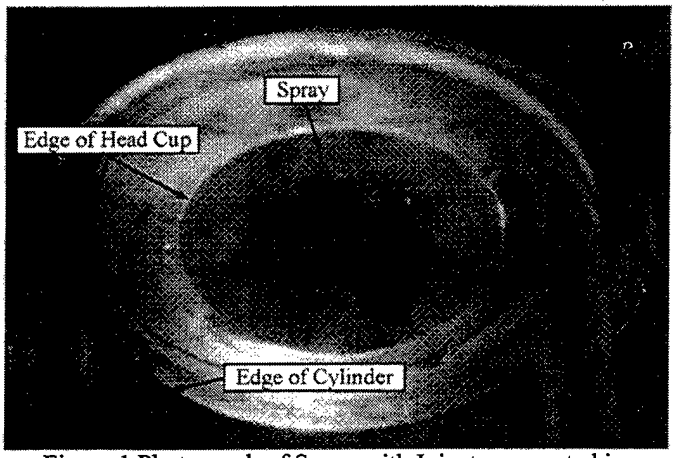

Figure 1 Photograph of Spray with Injector mounted in Cylinder Head

Figure 2 shows a schematic of the engine with the spray pattern that follows the cylinder head wall.

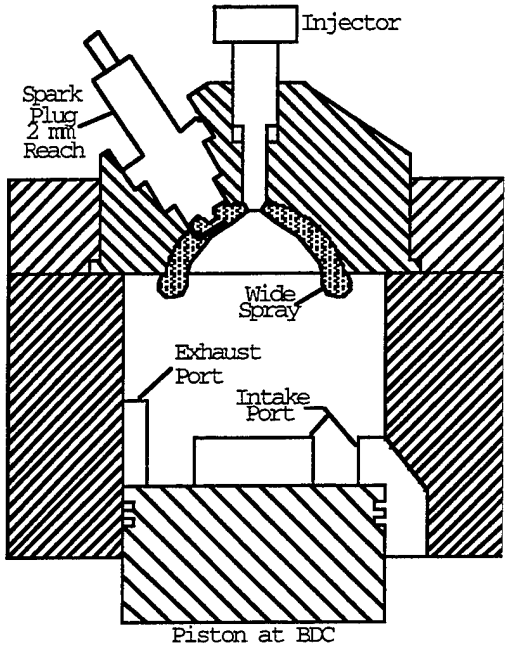

Figure 2 Schematic of Engine and Spray

Additional data demonstrating the degree to which the spray followed the wall of the hemispherical combustion chamber was obtained by mounting the head/injector assembly above a patternator in atmospheric conditions. The patternator consists of a single row of tubes (OD=2.5mm, ID=1.6mm) with a tube spacing of 3.9mm between centers. A detailed discussion of the patternator can be found in Ref. 8.

The liquid mass distribution measured by the patternator at the lower surface of the cylinder head is shown in Fig. 3 for injection quantities of 15 and 66 mm^3/injection. For reference, a cross-section of the hemispherical head is overlaid on the patternator results. From these data it can be seen that the fuel spray closely follows the chamber walls and suggest that 100 percent of the fuel is contained within 6.0 mm of the chamber surface. The data are relatively insensitive to the total mass of fuel injected.

The patternator used in these studies is also capable of making time-resolved measurements of the mass flux in the

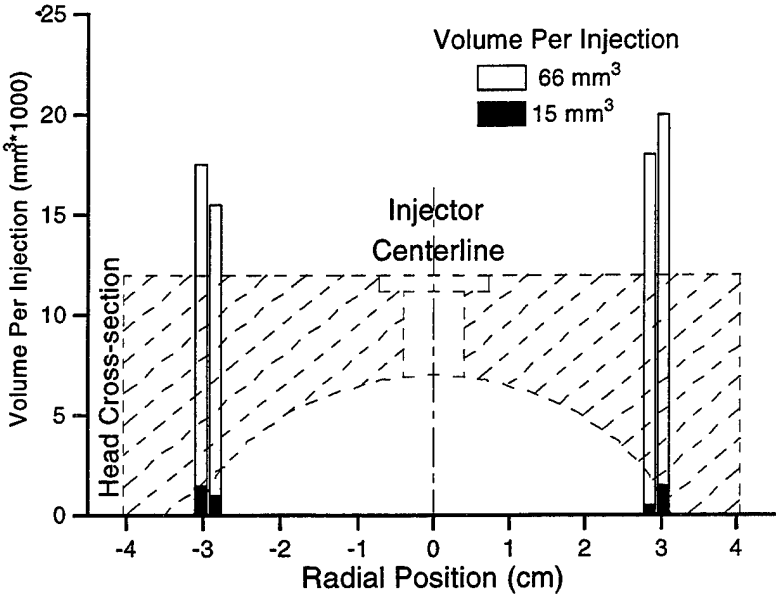

Figure 3 Spray Pattern Distribution Measured with Injector Mounted in Cylinder Head

spray. To accomplish this, the spray is passed through a rotating shutter. By phasing the pulsed injection with the shutter position, the tubes will only collect mass for a portion of the injection. By integrating the volume distribution obtained for different time segments, a curve representing the cumulative mass injected passing through a plane 1cm below the injector can be ascertained. The 1cm distance between the injector and measurement plane is required to accommodate the shutter mechanism. Fig. 4 shows the cumulative mass injected and poppet lift for the AFI injector.

These data were obtained for an injected volume of 69 mm^3 which is larger than would be typical for engine use, but was chosen to facilitate the data collection. The poppet lift data shows three distinct bounces, which is to be expected given the spring-mounted design, and is consistent with

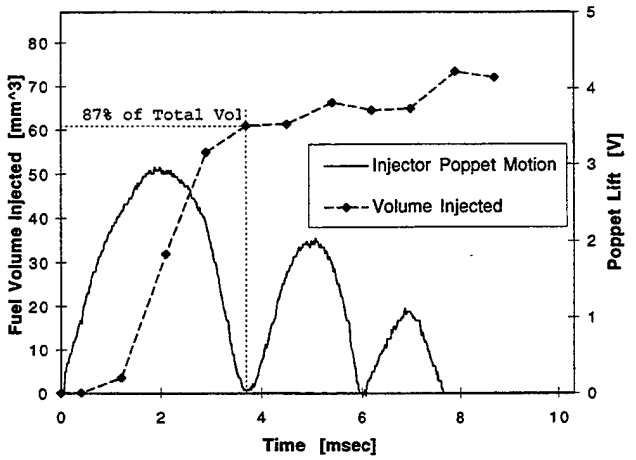

Figure 4 Injection Quantity Relative to Poppet Motion

previous findings. The cumulative volume indicate that very little liquid mass is injected in the first msec following poppet opening, but during the latter portion of the first poppet lift, 87% of the liquid mass is injected passes through the 1cm measurement plane. Thus, the majority of the liquid injection occurs during the latter portion of the first poppet lift. The later poppet motion should deliver air, and perhaps fuel vapor, but only a small proportion of the mass of liquid fuel. The total collected volume of the patternator was estimated to be 73 mm^3, which is approximately 5% higher than the known volume of fuel injected.

For the engine testing, a water-cooled piezoelectric pressure transducer (AVL 12QP300cvk piezoelectric transducer and Kistler 5004 charge amplifier) was used to record cylinder pressure. The cylinder pressure data was processed to calculate IMEP and net heat release for a set of 2000 cycles [9,10]. Exhaust emissions were measured from a sample probe located after a mixing tank in the exhaust system [11]. A heated sample line was used for a flame ionization detector (FID) hydrocarbon analyzer. This analyzer was calibrated with 6003 ppm propane (C_3H_8). A dry emission sample was produced by looping the exhaust sample line through an ice bath and condensing all the liquid out of the exhaust mixture. The dry sample was used to measure NOx (chemiluminescent analyzer), CO (NDIR analyzer), CO_2 (NDIR analyzer), and O_2 (polarographic analyzer).

The exhaust emission measurements from these analyzers was used to calculate the in-cylinder A/F ratio by several different procedures [12]. The values that were obtained from each of the methods were found to be consistent within 2%, so only the value calculated using the Bartlesville method will presented [13]. The fuel flow rate to the engine is necessary to convert the concentration measurements to a mass basis but could not be directly due the presence of the injector vent line. The fuel flowrate was estimated by:

$$\textit{Estimated Fuel Flow} = \frac{\textit{Measured Air Flow}}{\textit{A/F Ratio Estimated from Exhaust Composition}} \quad (1)$$

where the measured air flow is that delivered to the engine through the intake manifold, and does not account for the air delivered to the engine through the injector. The air delivered through the injector nozzle could not be measured due to the injector vent line. The fraction of the cylinder air that is delivered by the injector was estimated to be on the order of 5%. This underestimation of the total air delivered to the engine results in an equivalent underestimation of the estimated fuel mass flow. However, the estimated fuel flow rate was used for conversion of the emission measurements to a specific quantity, and thus, the absolute values of the specific emissions results should be used cautiously.

TEST CONDITIONS

Three speed/load conditions were investigated in this experiment in accordance with the typical duty cycle experienced in marine engines [14] and the emissions testing procedure suggested by the International Council of Marine Industry Associations (ICOMIA) [15]. The relationship between the engine load (torque) and speed for the five modes of the testing cycle is represented by the following function:

$$\frac{\textit{Boat Load}}{\textit{Engine Rated Torque}} = \left(\frac{\textit{Engine Speed}}{\textit{Rated Speed}}\right)^{1.5} \quad (2)$$

Table 2 lists the speed and torque values for each of the five testing modes. Operating Modes 2 (40% rated speed) and 3 (60% of rated speed) represent conditions that typically correspond to the transition between stratified combustion (under low speeds and loads) and homogeneous combustion (required for high speeds and loads).

For the current engine configuration, Mode 2 corresponds to a load of 9.6 N-m at a speed of 2000 RPM. Mode 3 corresponds to a load of 17.6 N-m at a speed of 3000 RPM, but due to speed limitations of the injector, the engine could not be operated at this speed. As a result, a speed of 2800 RPM with a boat load of 15.9 N-m was used instead. A third condition representing a high load condition at the lower speed was also chosen for investigation. The operating conditions are summarized in Table 3. During all the tests, the target exhaust A/F ratio was about 20:1. The A/F ratio was chosen because it would produce the lowest exhaust emission for stable running conditions. Ignition timing was fixed at 32 °BTDC for all the tests. Oil injection flow rate was 1/100th of the fuel flow by volume. A wide range of injection timings were used. The range of start of injection for each speed/load condition is listed in Table 4. The values reported for start of injection time are defined by the poppet lift reaching 40% full scale for the first poppet opening. The time between fuel injector opening and air solenoid opening was 100 degrees for 2000 RPM and 110 degrees for 2800 RPM.

Table 2 - ICOMIA Marine Duty Cycle

Mode	% Rated Speed	% Rated Torque	% Rated Power
1	Idle	0	0
2	40	25.3	10.1
3	60	46.5	27.9
4	80	71.6	57.2
5	100	100	100

Table 3 - Operating Conditions

	Units	Mode 2 Boat Load	Mode 2 High Load	Mode 3 Boat Load
Engine Speed	RPM	2000	2000	2800
Target Load	N-m	9.6	18.0	15.9
Power	kW	2.0	3.8	4.7
Measured Fuel Flow	kg/hour	1.01	1.45	1.82
Air Flow	kg/hour	16.7	25.7	32.6
Measured A/F	kg_{air}/kg_{fuel}	16.5	17.7	17.9
Exhaust A/F	kg_{air}/kg_{fuel}	19.9	20.4	21.1
Estimated Fuel Flow	kg/hour	0.83	1.25	1.55
Coolant Temp	°C	50	50	50
Oil injection ratio	Vol_{fuel}/Vol_{oil}	1/100	1/100	1/100
Ignition Timing	°BTDC	32	32	32
Injection Timing	°BTDC	205 - 51	180 - 59	232 - 98

Table 4 - Start of Injection Timing

Speed/Load Condition	Start of Injection Range
2000 RPM Boat Load	205 - 51 °BTDC
2000 RPM High Load	180 - 59 °BTDC
2800 RPM Boat Load	232 - 98 °BTDC

For this experiment, spark plugs with 3 different gap projections were used. Here, the spark gap projection is measured from the cylinder head wall to the center of electrode gap. An inductive ignition system was used for all the tests. Table 5 details the plugs that were used.

Table 5 - Spark Plug Gap Projections

Spark Plugs	Gap Projection
Short - NGK B6ES	0.7 mm
Medium - NGK BPR6ES	2.0 mm
Long - Champion RC10EOC	5.2 mm

RESULTS

The results section is organized as follows: First, shown in Fig. 5, is a complete depiction of the global engine combustion and emissions data. This is followed in Figs. 6-8 by detailed plots of results for specific operating conditions, in which individual cycle behavior is examined.

First, as shown in Fig. 5, for all three run conditions, there are optimum timings in terms of the magnitude of IMEP and the COV of IMEP. At 2000 rpm, this timing is for injector opening of 127° BTDC. It appears that the optimum timing for the higher speed is advanced slightly, to approximately 135° BTDC. The change in IMEP and COV of IMEP from the values obtained at this optimum timing are symmetrical with injection timing for both advanced and retarded timing. Again this is seen for all three operating conditions. Note that spark gap projection did not have a strong influence on these results.

Also illustrated in Fig. 5 are the BSNOx and BSHC results. The minimum in BSHC tends to occur at the optimum injection timing described above. However, for BSHC, there is a much stronger sensitivity to injection timing then observed in IMEP and COV of IMEP. In particular, there is an almost linear decrease in BSHC as the injection timing is retarded from the most advanced timing tested to the timing giving minimum BSHC. This would be expected if the amount of overmixing resulting in lean quench were dependent on the delay between injection and spark. For injection timings that are retarded from the timing producing the lowest BSHC, it is interesting that initially, the BSHC is nearly constant, until the most retarded timing, when it jumps suddenly to a high value. This behavior is consistent with the effects of misfire or partial burns. Again, note that spark gap projection did not have a strong influence on BSHC.

BSNOx results presented in Fig. 5 show the typical inverse relationship with BSHC. Such behavior with injection timing has been observed in other studies of the effect of injection timing on emissions in DI two-stroke engines [9,16]. However, in those studies the range of injection timing was approximately an order of magnitude smaller than what was used in this experiment.

More detailed combustion behavior for all three operating conditions are presented in Figs. 6-8. Results from three different injection timings (the most advanced timing, the injection timing producing the maximum value of IMEP, and the most retarded timing) have been included to illustrate the changes occurring in combustion with injection timing. For all the data shown in Figs. 6-8, the medium length gap

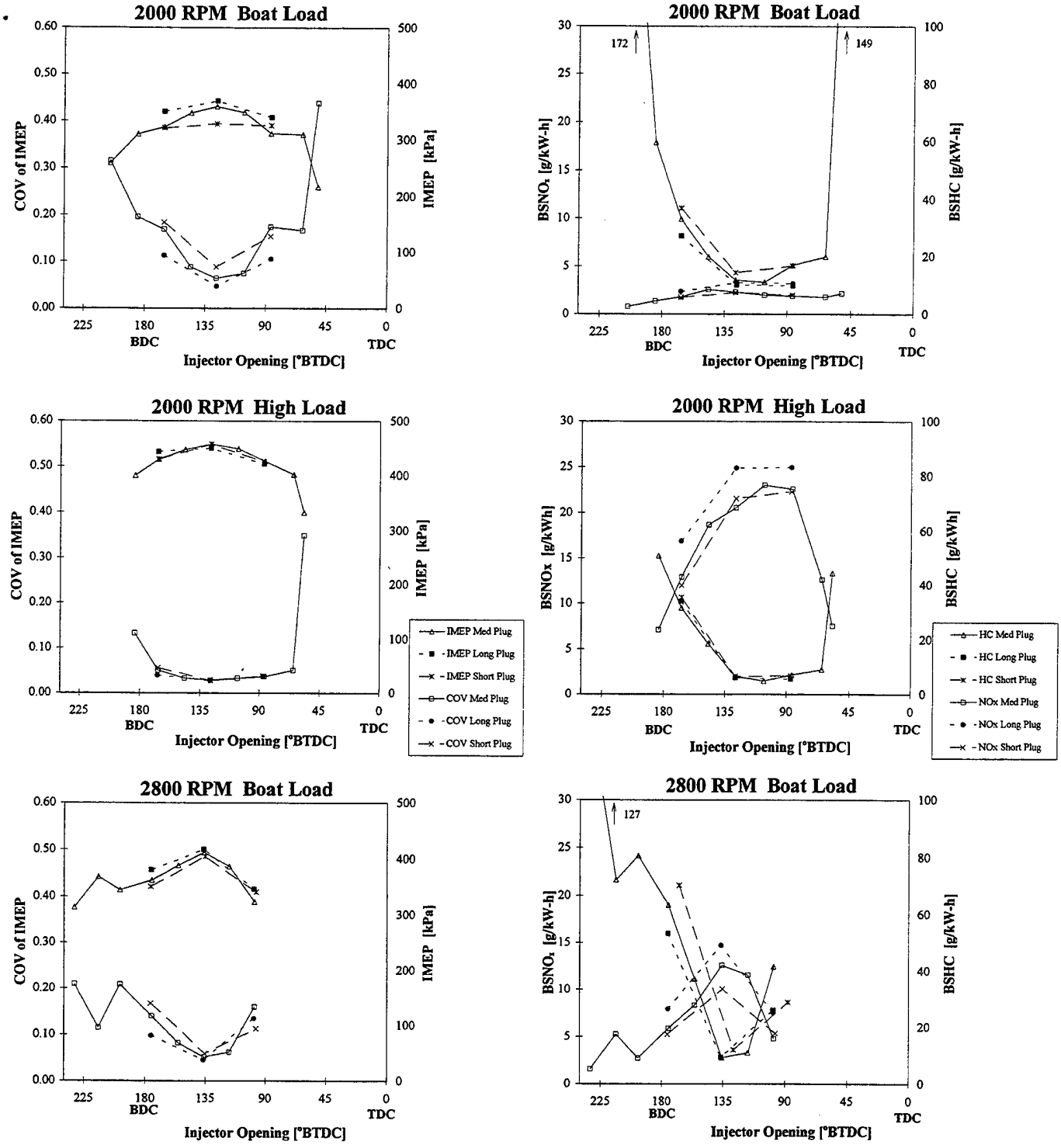

Figure 5 IMEP, COV, and Emission Measurements for 3 Speed/Load Conditions

(2mm) spark plug was used. Starting with the top row of figures, the most important observation is that the magnitude of cylinder pressure can strongly affect poppet motion. As shown, the most retarded injection timings are characterized by a single poppet opening event, instead of the three or four openings observed at the more advanced injector timings. The high cylinder density at retarded injection timings has been observed to produce significant changes in the behavior of unconfined hollow-cone sprays [6], but no data are available for the wall-stabilized configuration. However, the increased density at retarded timings is expected to further enhance the Coanda effect which is causing the spray jet to attach to the head surface at atmospheric conditions.

The second row in Figs. 6-8 compares the nature of cyclic variability produced. For the most advanced timings, there are two characteristics. The first is that there is little evidence of prior cycle interactions, indicating that all of the observed variations are a result of variations in burn within a

Figure 6: 2000 RPM Boat Load at Three Injection Timings

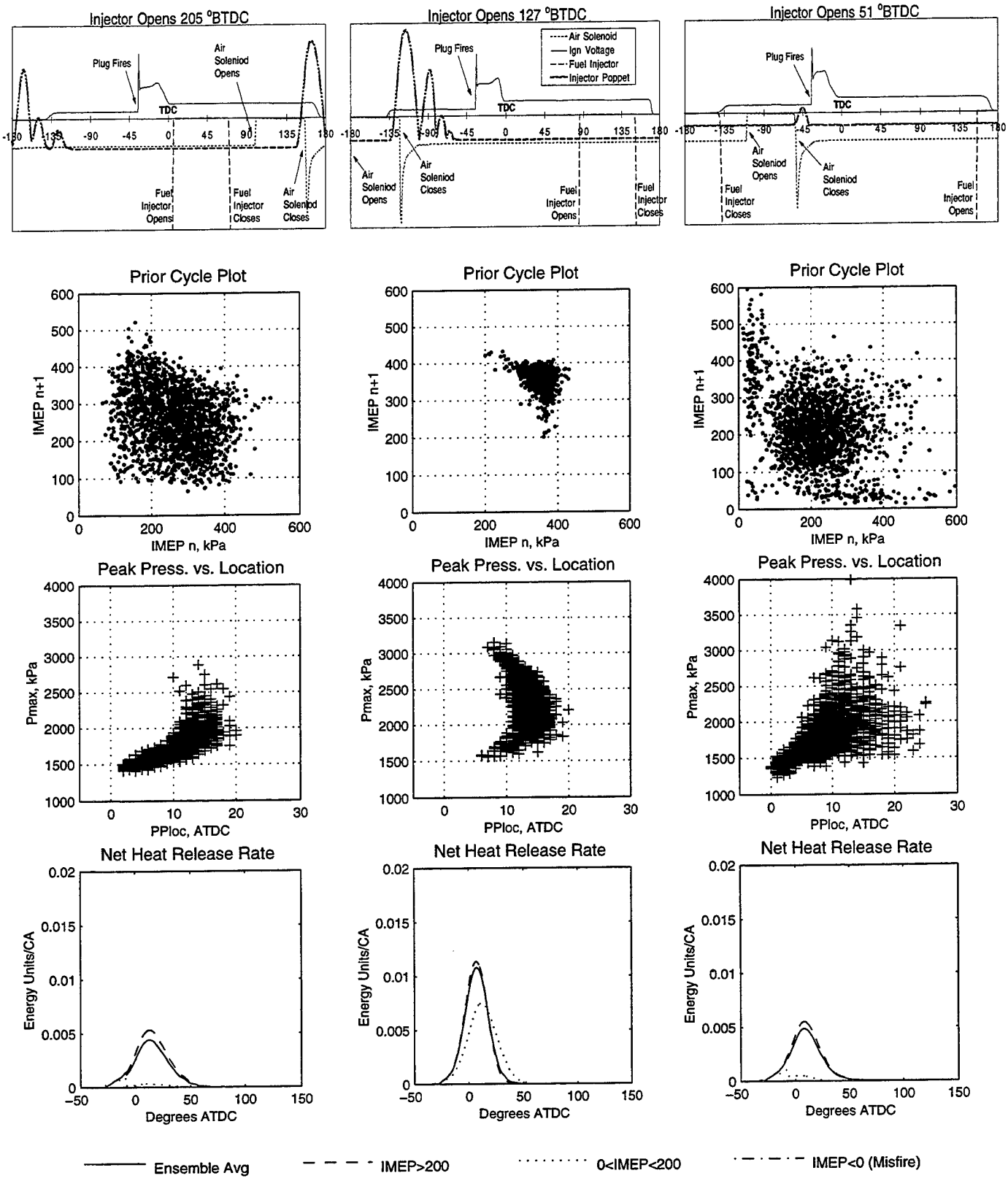

Figure 7: 2000 RPM High Load at Three Injection Timings

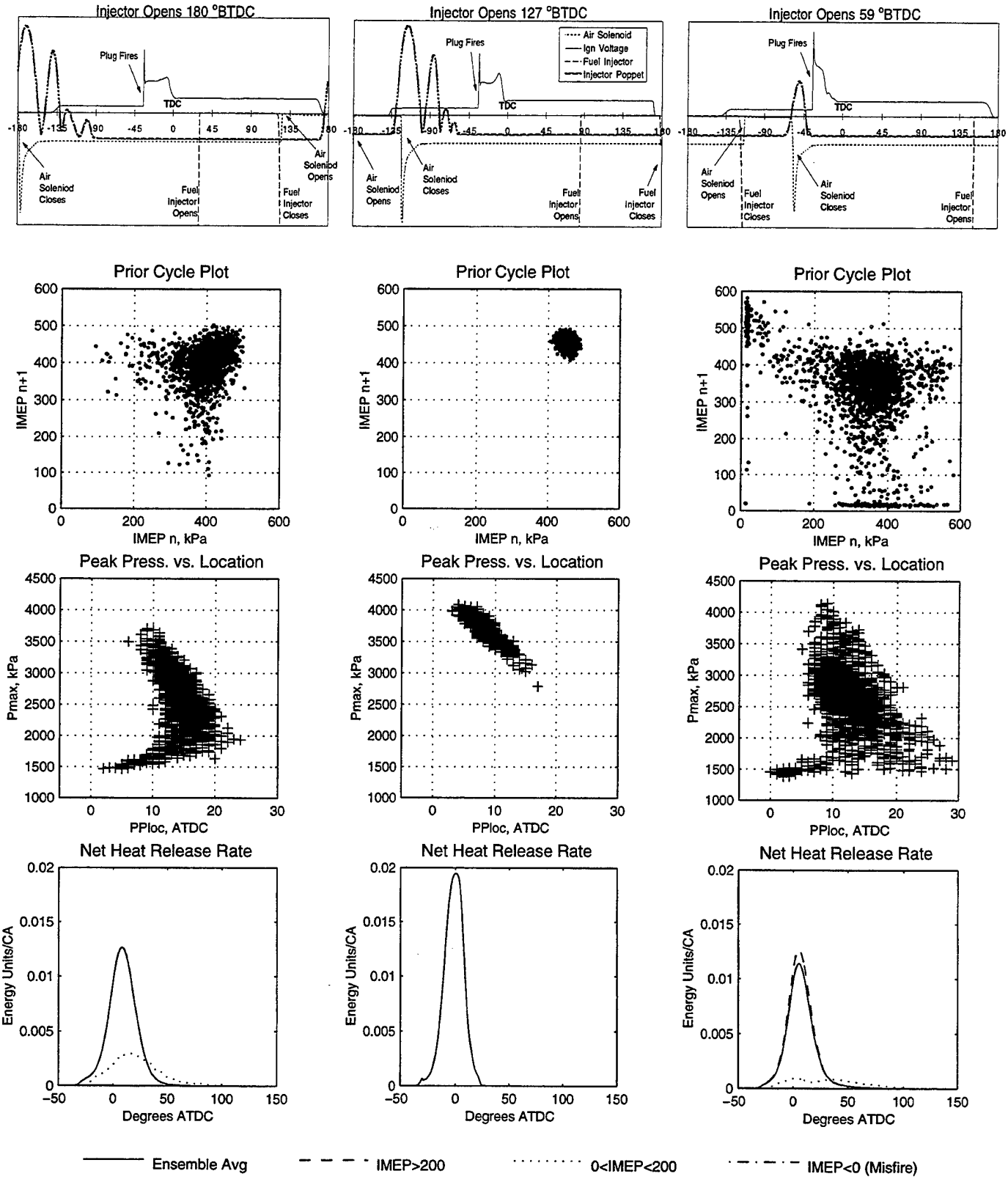

Figure 8: 2800 RPM Boat Load at Three Injection Timings

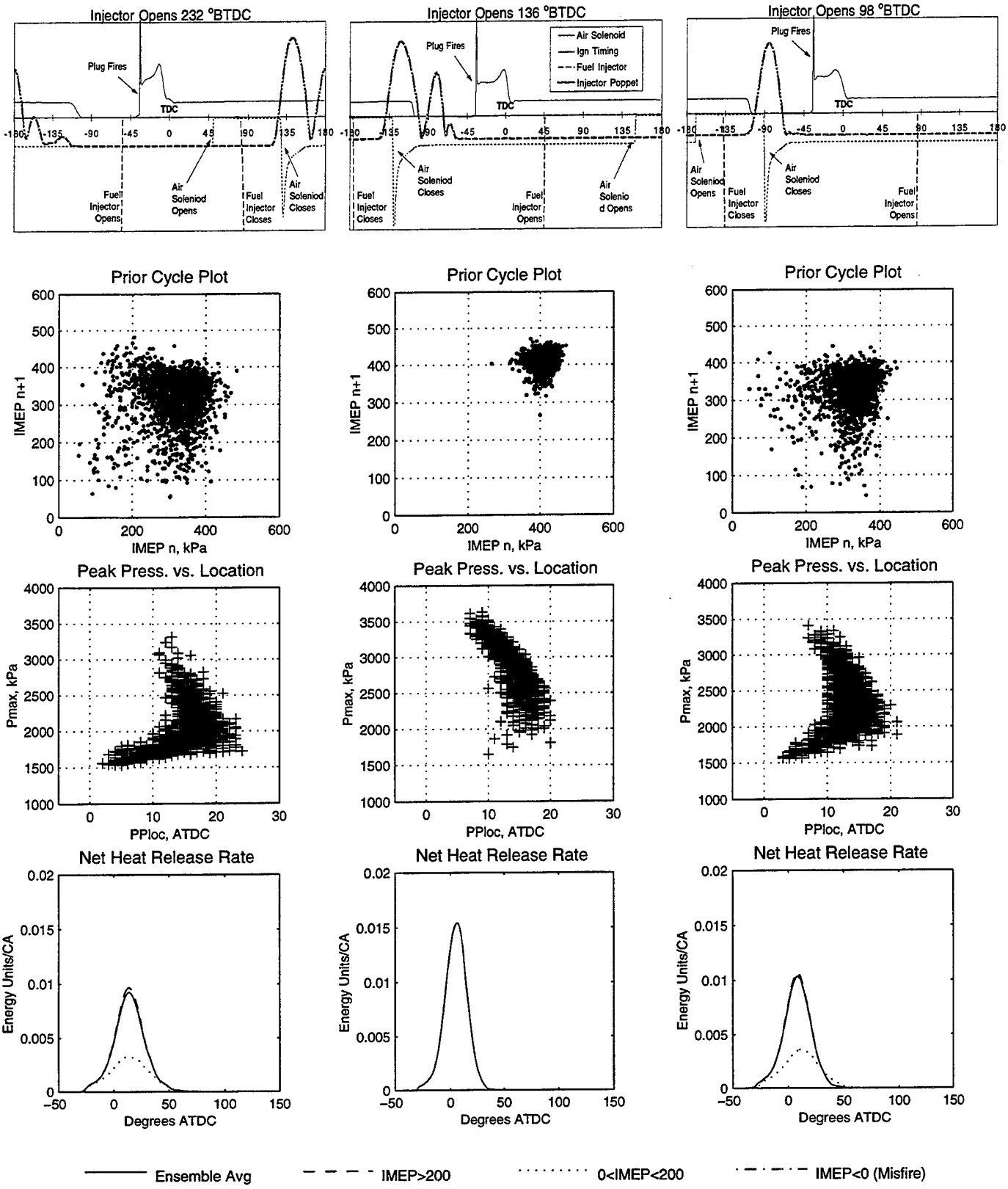

particular cycle [10]. The second is that there are no complete misfires. For injection timings producing maximum IMEP, there is little variation. In contrast, at the most retarded injection timings, there is strong evidence of interactions between cycles, consistent with partial burns or misfires. Finally, the 2000 rpm, high load operating condition shows evidence that the engine is frequently in a mode of successful combustion occurring once every two cycles. Such behavior is common in DI two-stroke engines with retarded injection timings.

Comparison of peak pressure and location of peak pressure is shown in the third row of Figs. 6-8. There appears to be major differences in the nature of the combustion process and rate with injection timing. For example, at the most advanced injection timings, the typical linear and hook-back relationship between burn phasing and peak pressure is displayed. In fact, at the most advanced injection timings studied, these plots are very similar to what is observed near the lean-limit in homogeneous charge 4-stroke engines [17]. In contrast, at the injection timings shown in the middle columns of Fig. 6-8, the variation all lies in the "linear" region, where the cyclic variation all appears to be a result of effective variation of ignition timing. Also at these injection timings, the highest peak pressures and apparent heat release rates are obtained. These timings appear to be optimum in terms of combustion rate and variability. The occurrence of such a optimum could be a results of several factors: 1) these may represent injection timing where there is optimum coupling between the spray momentum and in-cylinder gas flows. 2) These injection timings may result in equivalence ratio within the burning zone that have the highest flame speed. 3) These injection timings may result in combustion regimes that optimize equivalence ratio and minimize the flame travel distance required. Future studies will attempt to identify the dominant affects.

The most retarded timings tested produce indication of problems with consistent ignition, and indication that there has been inadequate time for mixing. This is evident by the trends in peak pressure and location of peak pressure, as well as the reduced peak heat release rates.

SUMMARY

Measurements have been obtained of direct-injection two-stroke engine combustion and emissions for the special case in which the spray behavior is influenced by the cylinder head bowl surfaces:

1) The combustion behavior indicates tolerance to a wide range of injection timings and spark locations. Emission measurements demonstrate the typical inverse relationship between BSHC and BSNOx for all cases tested.

2) For the advanced injection timings studied, the combustion behavior is characterized by variation consistent with homogeneous lean-burn combustion. BSHC peaked at the most advanced timings tested, and initially decreased as injection timing were retarded.

3) Injection timings which produce the highest IMEP also have the most stable and fastest combustion. BSHC is minimum at these timings, with a peak in BSNOx emissions.

4) The most retarded timings tested produce combustion behavior in which ignition is frequently not successful, and there are problems in completing the burn. At these timings, BSHC increases from the minimum with further retard in injection timings.

ACKNOWLEDGMENTS

Funding for this work was provided by the Wisconsin Small Engine Consortium (WSEC) and by the Department of Administration of the State of Wisconsin. The Engine Research Center is also supported by the Army Research Office through grant Nos. DAAH04-94-G-0328 and DAAHL03-92-0122. Thanks are also due to Ford Motor Company for providing the injection system used in this study.

REFERENCES

1. Syvertsen, M.L., Martin J.K., Hoffman J.A., Coates, S.W., McGinnity, F.A, *"Injection and Ignition Effects on Two-Stroke Direct Injection Emissions and Efficiency"*, SAE Paper No. 961803, Society of Automotive Engineers, Warrendale, PA, 1996

2. Schechter, M.M., and Levin, M.B., *"Air-Forced Fuel Injection System for 2-Stroke D.I. Gasoline Engine"*, SAE Paper No. 910664, Society of Automotive Engineers, Warrendale, PA, 1991.

3. Syvertsen, M.L., "*Two Stroke Direct Injection Emissions and Efficiency: A Statistical Approach*", M.S. Thesis, University of Wisconsin-Madison, 1996.

4. Emerson, J., Felton, P.G., Bracco, F.V., *"Structure of Sprays from Fuel Injectors Part III: The Ford Air-Assisted Fuel Injector"*, SAE Paper No. 900478, Society of Automotive Engineers, Warrendale, PA, 1990.

5. MacInnes, J.M., and Bracco, F.V., *"Computation of the Spray from an Air-Assisted Fuel Injector"*, SAE Paper No. 902079, Society of Automotive Engineers, Warrendale, PA, 1990.

6. Ghandhi, J.B., Felton, P.G., Gajdeczko, B.F., Bracco, F.V., *"Investigation of the Fuel Distribution in a Two-Stroke Engine with an Air-Assisted Injector"*, SAE Paper No. 940394, Society of Automotive Engineers, Warrendale, PA, 1994.

7. Ghandhi, J.B., and Bracco, F.V., *"Fuel Distribution Effects on the Combustion of a Direct-Injection Stratified-Charge Engine"*, SAE Paper No. 950460, Society of Automotive Engineers, Warrendale, PA, 1995.

8. Hoffman, J.A., Eberhardt, E., Martin, J.K., "*Comparison Between Air-Assisted and Single-Fluid Pressure Atomizers for Direct-Injection SI Engines Via Spatial and Temporal Mass Flux Measurements*", SAE Paper No. 970630, Society of Automotive Engineers, Warrendale, PA, 1997.

9. Rohrer, R., and Chehroudi, B., *"Preliminary Heat Release Analysis in a Single-Cylinder Two-Stroke Production Engine"*, SAE Paper No. 930431, Society of Automotive Engineers, Warrendale, PA, 1993.

10. Martin, J.K., Plee, S.L., and Remboski, D.J., *"Burn Modes and Prior-Cycle Effects on Cyclic Variations in Lean-Burn Spark-Ignition Engine Combustion"*, SAE Paper No. 880201, Society of Automotive Engineers, Warrendale, PA, 1988.

11. Society of Automotive Engineers, "*Test Procedure for the Measurement of Exhaust Emissions for Small Utility Engines* SAE J1088 JUN83", SAE Handbook, SAE, Warrendale, Pa; 1985, pp 25.148-25.153.

12. Myers, J., Myers, M., Myers, P., "*On the Computation of Emissions from Exhaust Gas Composition Measurements*", Journal of Engineering for Gas Turbines and Power, vol. III, pg. 410, 1989.

13. Chamberlain, T.W., Koehler, D.E., Stamper, K.B., and Marshall, W.F., *"Performance Characteristics of Automotive Engines in the U.S."* (Report No. 2), Energy Research and Development Administration, Bartlesville Energy Research Center report no. BERC/CP-77/47, August 1977.

14. Morgan, E.J., and Lincoln, R.H., "*Duty Cycle for Recreational Marine Engines*", SAE Paper No. 901596, Society of Automotive Engineers, Warrendale, PA, 1990.

15. Coates, S.W., and Lassanske, G.G., "*Measurement and Analysis of Gaseous Exhaust Emissions from Recreational and Small Commercial Marine Craft*", SAE Paper No. 901597, Society of Automotive Engineers, Warrendale, PA, 1990.

16. Private communication, Mercury Marine

17. Matekunas, F.A., *"Modes and Measures of Cyclic Combustion Variability"*, SAE Paper No. 830337, Society of Automotive Engineers, Warrendale, PA, 1983.